

# Synthesis and Characterization of Alkyl Imidazolium Based Periodic Mesoporous Organosilicas: A Versatile Host for the Immobilization of Perruthenate ( $\text{RuO}_4^-$ ) in the Aerobic Oxidation of Alcohols

Babak Karimi,<sup>\*,[a]</sup> Dawood Elhamifar,<sup>[a, b]</sup> Omolbanin Yari,<sup>[a]</sup> Mojtaba Khorasani,<sup>[a]</sup> Hojatollah Vali,<sup>[c]</sup> James H. Clark,<sup>[d]</sup> and Andrew J. Hunt<sup>[d]</sup>

**Abstract:** The preparation and characterization of a set of periodic mesoporous organosilicas (PMOs) that contain different fractions of 1,3-bis(3-trimethoxysilylpropyl)imidazolium chloride (BTMSPI) groups uniformly distributed in the silica mesoporous framework is described. The mesoporous structure of the materials was characterized by powder X-ray diffraction, transmission electron microscopy, and  $\text{N}_2$  adsorption–desorption analysis. The presence of propyl imidazolium groups in the

silica framework of the materials was also characterized by solid-state NMR spectroscopy and diffuse-reflectance Fourier-transform infrared spectroscopy. The effect of the BTMSPI concentration in the initial solutions on the structural properties (including morphology) of the final materials was also

**Keywords:** ionic liquids • mesoporous materials • organosilicas • perruthenate • supported catalysts

examined. The total organic content of the PMOs was measured by elemental analysis, whereas their thermal stability was determined by thermogravimetric analysis. Among the described materials, it was found that PMO with 10% imidazolium content is an effective host for the immobilization of perruthenate through an ion-exchange protocol. The resulting Ru@PI-10 was then employed as a recyclable catalyst in the highly efficient aerobic oxidation of various types of alcohols.

## Introduction

Since the first discovery of surfactant-templated ordered mesoporous silica by Beck et al.,<sup>[1,2]</sup> organically functionalized mesoporous silicas<sup>[3,4]</sup> have been extensively explored for applications that range from gas sorption, chromatography, and catalysis, to biological uses.<sup>[3–6]</sup> These materials exhibit a large specific surface area and narrow pore-size distribution that ranges from 2 to 30 nm. For most applications, the incorporation of organic groups inside ordered meso-

porous materials can normally be achieved through co-condensation of organotrialkoxysilanes  $[(\text{R}'\text{O})_3\text{Si}-\text{R}]$  with tetraalkoxysilanes in the presence of a suitable structure directing agent (SDA) to produce organofunctionalized ordered mesoporous materials.<sup>[3–6]</sup> In these types of materials, however, due to a loss or a significant reduction in the degree of long-range order, inhomogeneous distribution of organic groups in the pores, and partial filling of pore spaces by pendant organic groups, thereby restricting substrate diffusion into the channels, the organic content of these materials cannot exceed approximately 25 molar percent of the total silicon source.<sup>[7,8]</sup> To address these limitations, in 1999 a number of groups including Inagaki,<sup>[9]</sup> Stein,<sup>[10]</sup> and Ozin<sup>[11]</sup> independently discovered a new class of hybrid organic–inorganic materials called periodic mesoporous organosilicas (PMOs) built from bridge organosilica precursors,  $[(\text{R}'\text{O})_3\text{Si}-\text{R}-\text{Si}(\text{OR}')_3]$ , in which organic group R is an integral part of the mesoporous walls. In these materials, the bridging organic moieties in the framework of PMOs not only have improved hydrothermal and mechanical stabilities, but also higher organic loading and greater avoidance of channel blockage can be achieved relative to mesoporous materials functionalized with terminal organic groups.<sup>[7,8,12–14]</sup> These unique properties allow PMOs to be excellent candidates for widespread applications in material and chemical sciences.<sup>[7,8,12,13]</sup> In particular, depending on the nature of the organic species in the framework, the chemical and physical properties of PMOs can be tuned towards specific applications. These include a plethora of bridged organic units that have been uti-

[a] Prof. Dr. B. Karimi, Dr. D. Elhamifar, O. Yari, Dr. M. Khorasani  
Department of Chemistry  
Institute for Advanced Studies in Basic Sciences (IASBS)  
PO Box 45195-1159, Gava zang  
Zanjan, 45137-6731 (Iran)  
Fax: (+98) 241-4214949  
E-mail: karimi@iasbs.ac.ir

[b] Dr. D. Elhamifar  
Department of Chemistry, Yasouj University  
Yasouj, 75918-74831 (Iran)

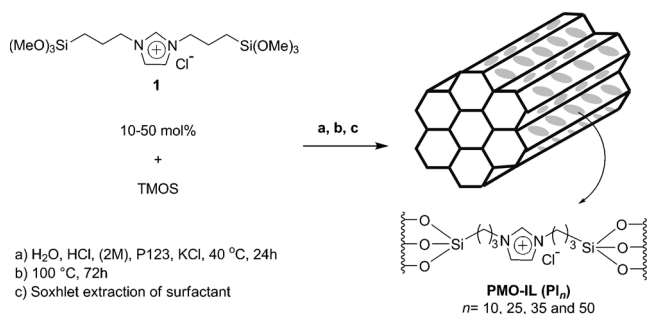
[c] Prof. H. Vali  
Anatomy and Cell Biology and Facility for  
Electron Microscopy Research, McGill University  
3450 University St, Montreal  
Quebec, H3A 2A7 (Canada)

[d] Prof. J. H. Clark, Dr. A. J. Hunt  
Green Chemistry Centre of Excellence  
University of York, York, YO10 5DD (UK)

Supporting information for this article is available on the WWW under <http://dx.doi.org/10.1002/chem.201200380>.

lized for the preparation of different types of PMOs with novel bulk properties, thus extending the concept of “pore chemistry” into the “wall chemistry” inside the hybrid mesoporous material world.<sup>[7,8,12,13,15–23]</sup>

Ionic liquids (ILs) have received great attention in recent years in a variety of areas that range from catalysis<sup>[24–27]</sup> and separation science to material synthesis as well as environmentally acceptable solvents for chemical reactions.<sup>[24–29]</sup> However, despite promising results, their widespread application in process chemistry is still hampered because many of them are very expensive and are a cause of toxicological concern.<sup>[30]</sup> Moreover, it is well known that the relatively high viscosity of the ionic liquids in many of the liquid–liquid biphasic reactions means that generally only a small fraction of the so-called “diffusion layer” of ILs participates in the overall reaction process.<sup>[31]</sup> Therefore, on account of the slow mass transfer of highly viscous liquids, it is indeed not necessary to use large amounts of ionic-liquid solvents. To address these limitations, the concept of supported ionic-liquid catalysis (SILC) has recently been introduced, which combines the advantages of ionic liquids with those of heterogeneous systems such as easy recyclability.<sup>[32–38]</sup> However, it has been shown that in many cases the ionic-liquid layer, which serves as the reaction phase, can be partially dissolved in the organic phase, thus restricting catalyst recovery.<sup>[32,33,39,40]</sup> Although drawbacks such as leaching can be partly avoided by designing various types of chemically supported ionic liquids,<sup>[41,42]</sup> the low loading of immobilized ionic liquid and their inhomogeneous distribution through inorganic supports are still important issues that remain unresolved. Considering the unique characters of PMOs, we recently prepared a novel PMO that contained 10% 1,3-bis(3-trimethoxysilylpropyl)imidazolium chloride (BTMSPCl) groups that were uniformly distributed in the silica mesoporous framework.<sup>[43]</sup> In our follow-up study herein, we wish to demonstrate the possibility of using a relatively wide range of concentration of BTMSPCl ionic liquids bound to the silica framework of the PMO materials.<sup>[44,45]</sup> The preparation of ionic-liquid-based periodic mesoporous organosilicas (PMO-IL) was achieved by co-condensation of 1,3-bis(3-trimethoxysilylpropyl)imidazolium chloride ionic liquid **1** and tetramethoxysilane (TMOS) in the presence of Pluronic P123 under acidic conditions (Scheme 1).



Scheme 1. Preparation of PMO-IL materials.

These materials showed remarkable thermal and structural properties over a relatively wide concentration range and synthetic conditions. The possibility of using these materials as an effective host for the immobilization of perruthenate in the aerobic oxidation of various types of alcohols is also investigated in some detail for the first time.

## Results and Discussion

Nitrogen adsorption–desorption and pore-size distribution isotherms of solvent-extracted PMO materials are shown in Figure 1.

The isotherms indicate that the pore sizes of all samples are in the mesoporous range. The organosilica materials showed typically type IV  $\text{N}_2$ -sorption isotherms with H1 or

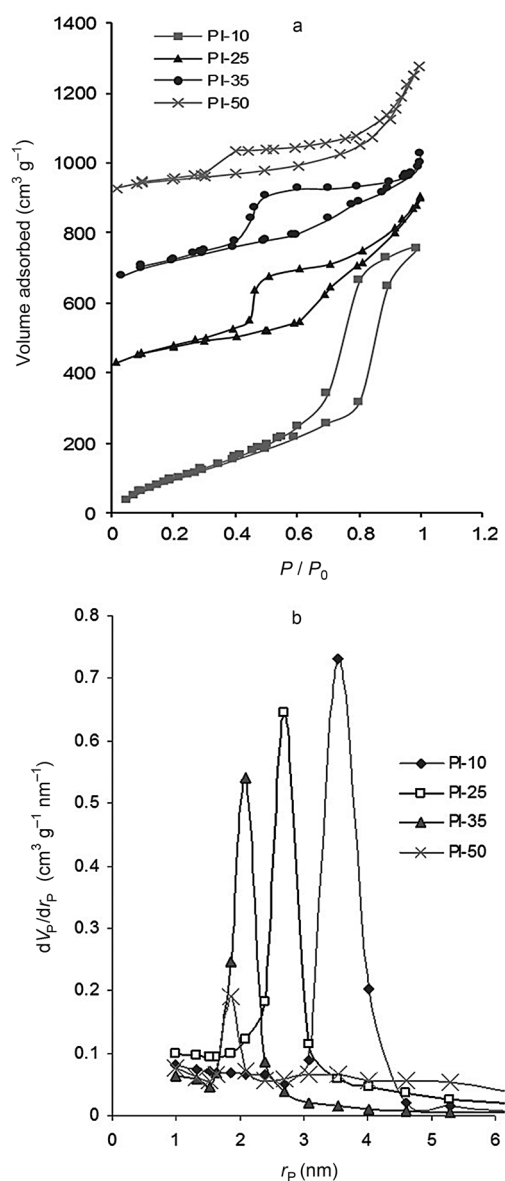


Figure 1. a) Nitrogen adsorption–desorption isotherms and b) pore-size distributions of the PMO-IL material.

H2 hysteresis loops according to the IUPAC classification, which is characteristic of mesoporous materials. In particular, N<sub>2</sub>-adsorption isotherms for PI-25 and PI-35 showed a broad hysteresis loop with a relatively sharp capillary condensation step at a relative pressure of approximately 0.70, and a very sharp capillary evaporation step centered at approximately 0.45, which is very close to lower limit of adsorption–desorption hysteresis. Since the course of the adsorption and desorption branches are not exactly parallel, “ink-bottle-like” pores should be considered to exist in both samples. Similar shapes of adsorption–desorption isotherms have been reported for FDU-1 and other PMOs or ordered silicas with large cage-like mesopores.<sup>[17,46]</sup> On the other hand, the shape of the resulting isotherms for PI-10 reveals a typical sharp hysteresis loop similar to those of SBA-15 type materials, thereby confirming a two dimensional (2D) hexagonal mesopore structure with a narrow pore-size distribution. For PI-10, PI-25, and PI-35, the Brunauer–Emmett–Teller (BET) surface areas were 671, 483, and 372 m<sup>2</sup> g<sup>−1</sup>; pore diameters were 7.0, 5.4, and 4.2 nm; and pore volumes 1.21, 0.82, and 0.63 cm<sup>3</sup> g<sup>−1</sup>, respectively (Table 1).

Table 1. Structural parameters of all synthesized mesoporous materials determined from nitrogen-sorption experiments.

| Sample | BET surface area<br>[m <sup>2</sup> g <sup>−1</sup> ] | Pore diameter<br>[nm] | Pore volume<br>[cm <sup>3</sup> g <sup>−1</sup> ] |
|--------|---|-----------------------|---|
| PI-10  | 671   | 7.0                   | 1.21  |
| PI-25  | 483   | 5.4                   | 0.82  |
| PI-35  | 372   | 4.2                   | 0.63  |
| PI-50  | 260   | 3.7                   | 0.45  |

In the case of PI-50, the isotherm indicates that the material is still highly porous with a surface area of 260 m<sup>2</sup> g<sup>−1</sup>, and a pore volume of 0.45 cm<sup>3</sup> g<sup>−1</sup> (Table 1). The average pore diameter of PI-50, calculated from the adsorption branch of the isotherm using the Barrett–Joyner–Halenda (BJH) method, showed a broad pore-size distribution with pronounced maxima at 3.7 nm (Table 1). This indicates that both pore volume and the long-range order of the materials strongly decrease with increasing the concentration of bisilylated ionic liquid in the primary gel. A sharp rise in the isotherm for PI-25, PI-35, and PI-50 occurs at a relative pressure higher than 0.8, and this increase intensifies with increasing concentration of BTMSPI, which features in the gradual development of textural mesoporosity.

Powder X-ray diffraction (PXRD) analyses were performed on both as-prepared composites and the surfactant-extracted PMOs. The PXRD pattern of the as-made products showed a weak diffraction peak with low-intensity at  $2\theta \approx 1.1$ – $1.4$  (Figure S1 in the Supporting Information), thus reflecting a low electronic contrast between the inside of the channels and walls. On the other hand, all surfactant-extracted samples exhibit a single prominent peak in the diffraction pattern at approximately the same region as those of the as-prepared materials, which is characteristic of materials with long-range periodicity (Figure S9 in the Supporting Information). This single peak is indexed as the  $d_{100}$  re-

flection and is usually observed for hexagonally ordered mesoporous materials. The results of  $d_{100}$  reflections and nitrogen adsorption–desorption analyses of the as-prepared and solvent-extracted PMOs indicate outstanding solvothermal stability, because none of the samples exhibited any appreciable matrix contraction upon surfactant extraction. Another interesting observation was that by increasing the concentration of IL in the initial gel, the intensity of the diffraction peak gradually decreased, thereby confirming the loss of structure ordering, as suggested from N<sub>2</sub> adsorption–desorption studies. This effect and also the absence of higher-order reflections ( $d_{110}$  and  $d_{200}$  reflections) can be attributed to either the large size of IL groups, which restrict their incorporation in the mesoporous walls, or the interference of initial BTMSP ionic liquid at higher concentration in the structure of the surfactant-template assembly. The appearance of one broad peak in the small-angle regions of the diffraction pattern of PI-50 is also supported by transmission electron microscopy, in which a relatively amorphous mesopore structure was observed but with no significant meso-scale ordering (see above).

Thermogravimetric analyses (TGA) of the PMO-IL samples were conducted in temperatures that ranged from 20 to 800 °C under air flow (Figure S2 in the Supporting Information). The first weight loss of about 4–8 % appeared around 100 °C, which corresponded to desorption of water and alcoholic solvents that remained from the solvent-extraction processes. The relatively large amount of water ( $\approx 8$  %) in samples PI-25, PI-35, and PI-50 might also suggest that alkyl imidazolium groups are well enclosed within the walls by the surrounding hydrophilic Si–OH moieties. It is well known that weight loss at 200–250 °C might generally be attributable to the decomposition of the residual surfactant. The absence of any significant weight loss in this range for the solvent-extracted PMO samples indicated that the surfactant was successfully removed by means of solvent extraction. The main weight loss (from 10.6 % for PI-10 to 39.7 % for PI-50), which was observed around 350 to 450 °C, with the same pattern, might be attributed to the thermal dissociation of the alkyl imidazolium groups. Another interesting observation is the broadening of the decomposition range that starts at 450 °C. This might be attributed to a partial transformation of bridge ionic-liquid groups with two-point attachment in the framework to ionic-liquid groups with single-point attachment. The amount of the incorporated alkyl imidazolium moieties into the framework of the material that was determined by elemental analysis showed a good agreement with the amount of organic groups estimated from the TGA data (Table 2). A comparison between

Table 2. Elemental analysis (EA) and TGA weight-loss data of the PMO-IL materials with different loading of ionic liquid.

| Sample | IL [mol %] | C [%] | N [%] | TGA weight loss [%] |
|--------|------------|-------|-------|---------------------|
| PI-10  | 10         | 14.0  | 3.4   | 10.6                |
| PI-25  | 25         | 19.4  | 5.0   | 24.5                |
| PI-35  | 35         | 22.7  | 6.1   | 29.2                |
| PI-50  | 50         | 24.6  | 6.7   | 39.7                |

carbon atoms found and calculated values shows that about 90% of the ionic liquid in the original mixture is incorporated into the organosilica framework, most likely because of the faster condensation rate of the tetramethoxysilane.<sup>[47]</sup>

The presence of alkyl-imidazolium moieties into the mesoporous network was identified by diffuse-reflectance infrared Fourier transform spectroscopy (DRIFTS) (Figure S10 in the Supporting Information). All synthesized samples display very similar DRIFT spectra with differences only in the relative band intensities. The two sharp and broad peaks at 1090 and 925 cm<sup>-1</sup> are attributed to the asymmetric and symmetric stretching vibration of the Si-O-Si in the framework.<sup>[22]</sup> In addition, all PMO materials show absorption peaks at 3125 cm<sup>-1</sup> (for unsaturated C-H stretching); 3050, 2918 cm<sup>-1</sup> (aliphatic C-H stretching); 1620 cm<sup>-1</sup> (C=N stretching of imidazolium ring);<sup>[47]</sup> 1558 cm<sup>-1</sup> (C=C stretching of imidazolium ring); 1442 cm<sup>-1</sup> (C-H deformation vibrations); 700–790 cm<sup>-1</sup> (for C-Si stretching vibrations); and also a broad peak around 3300 cm<sup>-1</sup> (stretching vibration of O-H groups), respectively.<sup>[22,42,48,49]</sup> Furthermore, the increase in intensity of absorption bands as the amount of IL increases confirms the structure and stability of IL groups during the processes of material synthesis and extraction.

The <sup>29</sup>Si and <sup>13</sup>C cross-polarization magic angle spinning (CP/MAS) NMR spectra of all mesoporous organosilica samples were also recorded to confirm the presence of IL in the mesoporous framework (Figure 2 and Figure 3; also see the Supporting Information for further images). The <sup>29</sup>Si NMR spectra of the all PMO materials display three signals at  $\delta = -49.5$ ,  $-58.5$ ,  $-67.5$  ppm, which correspond, respectively, to T<sup>1</sup> [C-Si-(OSi)(OH)<sub>2</sub>], T<sup>2</sup> [C-Si-(OSi)<sub>2</sub>(OH)], and T<sup>3</sup> [C-Si-(OSi)<sub>3</sub>] sites for Si species that are covalently bonded to carbon atoms. In addition, the <sup>29</sup>Si NMR spectra show three peaks at  $\delta = -111$ ,  $-102$ , and  $-91.5$  ppm, which correspond to the Q<sup>4</sup> [Si-(OSi)<sub>4</sub>], Q<sup>3</sup> [Si-(OSi)<sub>3</sub>(OH)], and Q<sup>2</sup> [Si-(OSi)<sub>2</sub>(OH)<sub>2</sub>] species of the silica framework, respectively. The degree of framework condensation was found to be high, as observed from the presence of a higher percentage of fully cross-linked T<sup>3</sup> and Q<sup>4</sup> silicon sites. Comparison of the solid-state <sup>29</sup>Si NMR spectra (Figure 2 and Table 3) shows that with increasing ionic liquid content in the initial gel, the intensity of T<sup>n</sup> bands with respect to Q<sup>n</sup> bands gradually increased, which illustrates the successful condensation and incorporation of IL moieties into the mesoporous walls.

The <sup>13</sup>C CP/MAS NMR spectra of all PMO materials show the characteristic signals of the alkyl-imidazolium bridging groups (Figures S3–S5 in the Supporting Information). For example, Figure 3 shows the solid-state <sup>13</sup>C NMR spectrum of PI-35, which can be assigned to the C species as follows:  $\delta = 10.0$  (SiCH<sub>2</sub>), 24.6 (CH<sub>2</sub>CH<sub>2</sub>CH<sub>2</sub>), 52.5 (CH<sub>2</sub>N), 123.2 (CHCH), and 136.0 ppm (NCHN). The absence of <sup>13</sup>C NMR spectroscopic resonances that correspond to the methoxy groups of the ionic-liquid organosilica precursor further confirms a high degree of hydrolysis and efficient cross-linking in the material. This is in good agreement with the results obtained from elemental analysis. These solid-

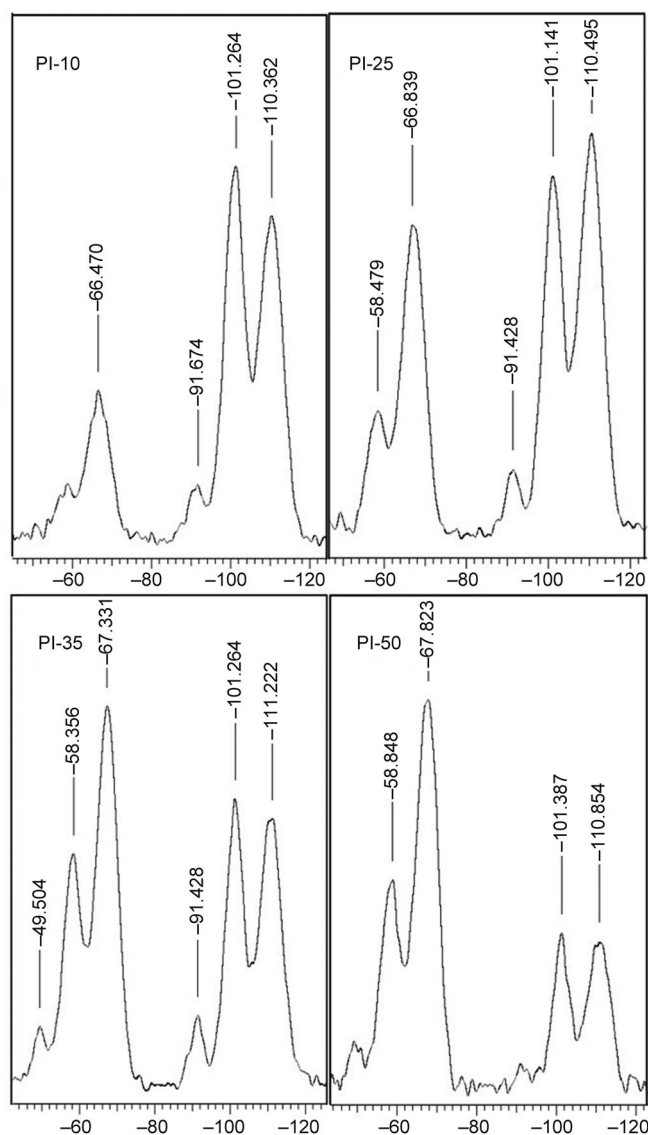
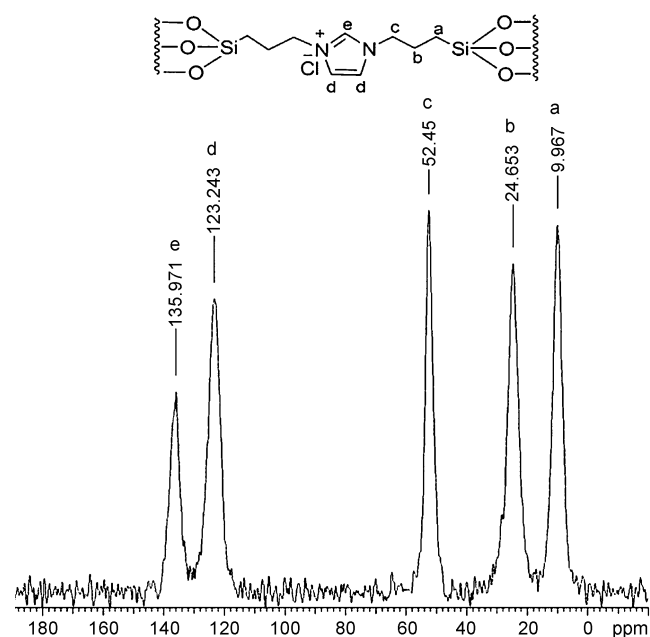


Figure 2. Solid-state <sup>29</sup>Si MAS NMR of materials PI-10, PI-25, PI-35, and PI-5.

state <sup>13</sup>C NMR spectra show that the ionic-liquid groups were indeed thoroughly incorporated into the mesoporous channel walls. Moreover, the lack of any further carbon resonance clearly shows that almost all Si-C bonds survived intact during the acidic polycondensation and the hot-solvent-extraction processes. Furthermore, the absence of surfactant peaks, which are located at  $\delta = 30$  and 70 ppm in the <sup>13</sup>C NMR spectra of surfactant-extracted samples, indicates complete removal of the surfactant under the extraction conditions.

In a separate experiment and for the purposes of comparison, we also prepared a sample of pure self-assembled ionic-liquid phase (SAILP; PI-100) through co-condensation of 1,3-bis(3-trimethoxysilylpropyl)imidazolium iodide (BTMSPI) under the same acidic conditions but in the absence of pluronic P123. The SAILP solid was also characterized by simultaneous thermal analysis and solid-state NMR



Figure 3. Solid-state  $^{13}\text{C}$  MAS NMR of PI-3.Table 3. Solid-state  $^{29}\text{Si}$  NMR spectroscopic data of PMO-IL materials.

| Sample | Q <sup>4</sup> [%] | Q <sup>3</sup> [%] | Q <sup>2</sup> [%] | T <sup>3</sup> [%] | T <sup>2</sup> [%] | T <sup>1</sup> [%] |
|--------|--------------------|--------------------|--------------------|--------------------|--------------------|--------------------|
| PI-10  | 41.2               | 29.3               | 5.0                | 44.9               | 11.0               | 1.7                |
| PI-25  | 29.9               | 24.1               | 3.7                | 27.4               | 13.1               | 1.9                |
| PI-35  | 23.5               | 21.9               | 4.3                | 32.2               | 16.2               | 1.9                |
| PI-50  | 17.3               | 12.7               | 1.9                | 43.0               | 21.6               | 3.4                |

spectroscopy. The uniform distribution of the alkyl imidazolium group in the silica framework of the material was confirmed by  $^{29}\text{Si}$  and  $^{13}\text{C}$  CP/MAS NMR spectroscopy.

The  $^{29}\text{Si}$  spectrum of the SAILP displays three signals at  $\delta = -49.1$ ,  $-58.52$ , and  $-68.36$  ppm, which correspond to T<sup>1</sup> [C–Si(OSi)(OH)<sub>2</sub>], T<sup>2</sup> [C–Si(OSi)<sub>2</sub>(OH)], and T<sup>3</sup> [C–Si(OSi)<sub>3</sub>] sites, respectively, for Si species that are covalently attached to carbon atoms (Figure S8 in the Supporting Information). In addition, the absence of any resonances at  $\delta = -90$  to  $-115$  ppm that are attributed to Q<sup>n</sup> sites of the silica framework clearly shows that no C–Si bond cleavage of the BTMSPI molecules occurred in the synthesis conditions of SAILP (Figure S8 in the Supporting Information). The solid-state  $^{13}\text{C}$  CP/MAS NMR spectrum of SAILP was also measured to clarify the characteristic signals of the alkylimidazolium bridging moieties in pure self-assembled ionic-liquid phase (Figure S7 in the Supporting Information). This spectrum illustrates carbon signals of the ionic liquid moieties as follows:  $\delta = 10.5$  (SiCH<sub>2</sub>), 24.7 (CH<sub>2</sub>CH<sub>2</sub>CH<sub>2</sub>), 52.8 (CH<sub>2</sub>N), 123.6 (CHCH), and 136.7 ppm (NCHN). This data also suggests that the ionic-liquid groups were well incorporated into the material network. Moreover, the absence of any other carbon signals confirms that almost all of the Si–C bonds survived intact under the synthesis conditions. Thermogravimetric analysis of the SAILP composite was also conducted from room temperature to 900 °C for purposes of comparison (Figure S6 in the Supporting Information).

TEM images of the solvent-extracted materials also provided further evidence that the structural integrity of the materials was retained after extraction of the template, a result consistent with the PXRD results and N<sub>2</sub>-sorption data. TEM images of PI-10 sample along different directions shows 2D hexagonal symmetry throughout the sample with superior uniformity in its framework (Figure 4a,b). TEM images of PI-25 and PI-35 also show a uniform rod structure with regularity in their channels (Figure 4c,d). However, TEM images of PI-50 show a wormhole motif structure (Figure 4e) that is consistent with a low degree of structural ordering as also evidenced by PXRD and N<sub>2</sub>-sorption analyses.

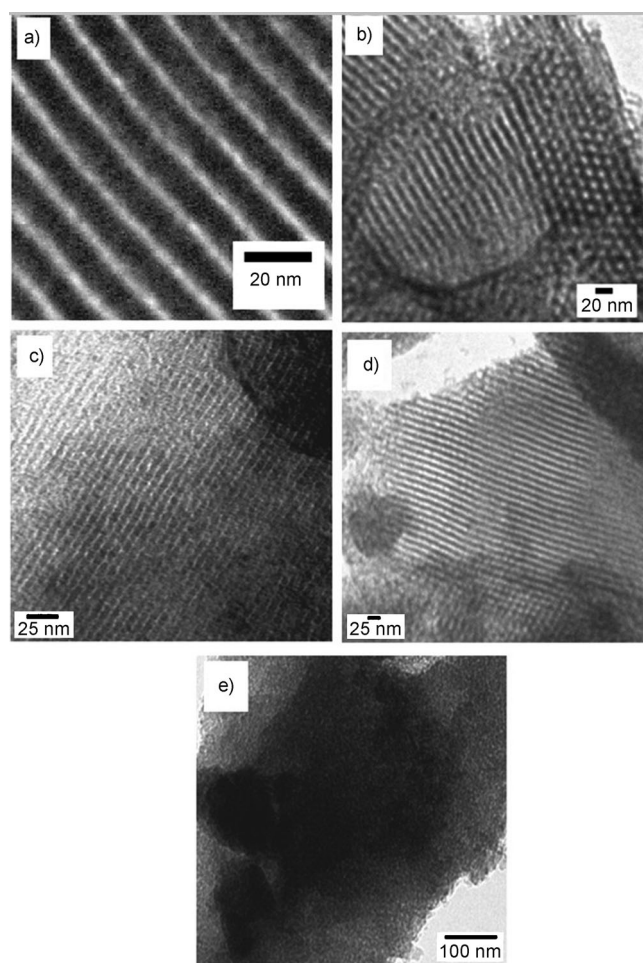


Figure 4. TEM images of materials a,b) PI-10, c) PI-25, d) PI-35, and e) PI-5.

SEM images of surfactant-extracted materials display well-defined external morphology (Figure 5). These images show that with increasing IL in the synthesized materials, a gradual change in the particle morphology could be observed. This change is from ropelike for PI-10 to sharp-edged particles for PI-50. PI-10 displays a ropelike structure with superior regularity and a diameter of 2–4  $\mu\text{m}$ .<sup>[19]</sup> PI-25 and PI-35 samples show a uniform spherical organosilica

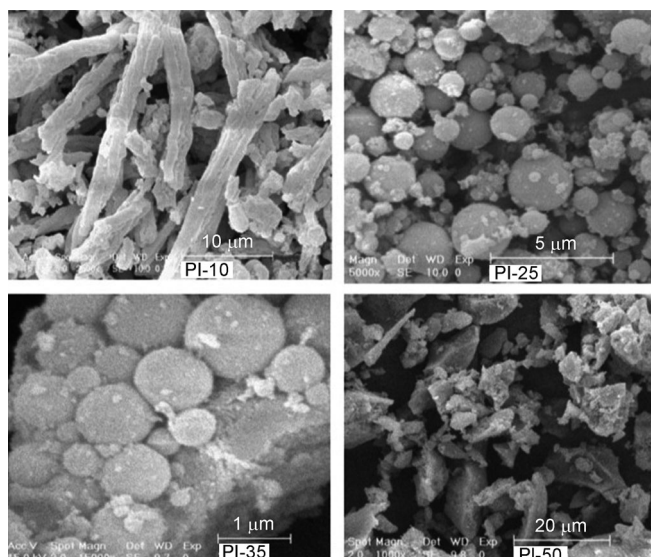
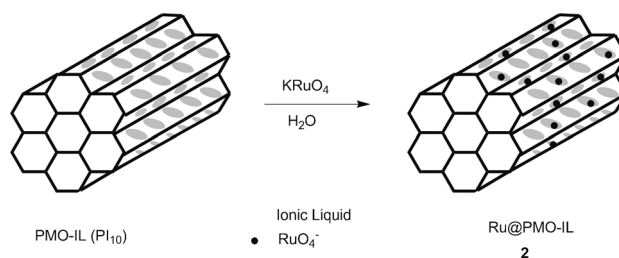


Figure 5. SEM images of materials PI-10, PI-25, PI-35, and PI-50.

with diameters that range between 0.5 and 2  $\mu\text{m}$ . These spherical mesostructures would be good candidates for chromatography, catalysis, and microelectronics applications due to their high uniformity and density.<sup>[50,51]</sup> The PI-50 sample consisted of isolated and also agglomerated particles with different shapes and sizes.

**Application in catalysis:** As the initial objective of this research was to develop PMOs with variable degrees of ionic-liquid moieties for application in catalyst immobilizations, we then turned our attention to the use of these materials as supports to begin the development of a wide variety of novel immobilized catalyst systems. In an earlier communication, we demonstrated that among different types of functionalized organosilicas, self-assembled organic–inorganic hybrid silica with an alkylimidazolium bridge (SAILP; PI-100) was better suited as a support to immobilize a Yb(OTf)<sub>3</sub>–pybox (pybox = 2,6-bis[(4R)-4-phenyl-2-oxazolinyl]–pyridine) complex in catalyzing the enantioselective addition of trimethylsilyl cyanide (TMSCN) to aldimines.<sup>[52]</sup> We have also investigated the ability of mesoporous organosilicas for actual use as a support for the immobilization and stabilization of Pd nanoparticles in the Suzuki-coupling reaction of aryl halides with arylboronic acids<sup>[43]</sup> and the aerobic oxidation of a diverse range of alcohols under mild reaction conditions.<sup>[53]</sup> In these studies, we found that the PMO-IL nanostructure could indeed act as a nanoscaffold to stabilize Pd nanoparticles (PdNPs) in the mesochannels, thus preventing undesired agglomeration of Pd nanoparticles. In continuation of these studies, we therefore speculate that this innovative system with tunable loading of imidazolium moieties could be used as a support in a very similar way to the preparation of a novel ruthenium-supported catalyst through the anion exchange of  $\text{RuO}_4^-$  with chloride anions inside the PMO-IL framework, which is denoted as Ru@PMO-IL **2** (Scheme 2). In this regard, we chose to



Scheme 2. Preparation of Ru@PMO-IL **2**.

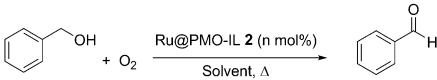
employ PI-10 as the support, because of our previously successful experience in preparing several catalytic systems based upon this material.<sup>[43,53]</sup>

The selective oxidation of alcohols to carbonyl compounds is a key process in organic synthesis and plays a crucial role in the fine chemicals industries. There is a plethora of stoichiometric oxidizing reagents to selectively effect this transformation.<sup>[54]</sup> These oxidizing reagents are, however, often very expensive and there are sometimes serious toxicity concerns associated with them. Therefore, the oxidation of alcohols by using molecular oxygen or air in the presence of a recyclable heterogeneous catalyst system offers significant advantages from both environmental and economic points of view.<sup>[55]</sup> In this context, several supported catalysts based upon Pd,<sup>[56]</sup> Au,<sup>[57]</sup> Pt,<sup>[58]</sup> and Ru<sup>[59]</sup> were found to show interesting activity in the aerobic oxidation of alcohols. Although a significant number of these catalyst systems have given remarkable results in terms of selectivity and substrate scope, in many cases, they are not suitable for non-activated alcohols such as aliphatic and alicyclic alcohols. Moreover, many of the catalysts can produce satisfactory yields of products only in the presence of large excess amounts of base additives.<sup>[56,57]</sup> Among the various heterogeneous catalysts exploited so far, ruthenium-based catalysts show promising catalytic performances because they not only catalyze the aerobic oxidation of alcohols in the absence of base additives,<sup>[59]</sup> but also offer excellent catalytic activities in a variety of other important functional-group transformations.<sup>[60]</sup>

The aerobic oxidation of benzyl alcohol to benzaldehyde was used to probe the catalytic activity of Ru@PMO-IL.<sup>[61]</sup> First, we examined the aerobic oxidation of benzyl alcohol (1 mmol) by using molecular oxygen (1 atm) in the presence of 5 mol % of **2**, in toluene (2 mL) at room temperature. Under these conditions, 53 % of the corresponding aldehyde was obtained after 72 h (Table 4, entry 1).

The same reaction at 50 °C smoothly went to completion within 16 h to afford an excellent yield of 99 % of benzaldehyde as the sole product (Table 4, entry 2). The reaction was further optimized for the reaction temperature, and we found that by increasing the reaction temperature to 70 °C, the reaction proceeded more readily and the desired aldehyde was obtained in almost quantitative yields after 9 h (Table 4, entries 1–4).

Investigation of the impact of catalyst loading, reaction solvents, and the temperature revealed that a catalyst load-

Table 4. Effects of catalyst loading, solvent, and reaction temperature on the aerobic oxidation of benzyl alcohol catalyzed by Ru@PMO-IL **2**.<sup>[a]</sup>


| Entry     | <i>n</i>   | Solvent          | <i>T</i> [°C] | <i>t</i> [h] | Yield [%] <sup>[b]</sup> | TOF [h <sup>-1</sup> ] |
|-----------|------------|------------------|---------------|--------------|--------------------------|------------------------|
| 1         | 5          | toluene          | RT            | 72           | 53                       | 0.14                   |
| 2         | 5          | toluene          | 50            | 16           | > 99                     | 1.23                   |
| 3         | 5          | toluene          | 60            | 13           | > 99                     | 1.52                   |
| 4         | 5          | toluene          | 70            | 9            | > 99                     | 2.24                   |
| 5         | 2.5        | toluene          | 70            | 14           | > 99                     | 2.80                   |
| 6         | 5          | THF              | RT            | 72           | 20                       | 0.05                   |
| 7         | 5          | H <sub>2</sub> O | RT            | 72           | 14                       | 0.04                   |
| 8         | 5          | H <sub>2</sub> O | 70            | 72           | 17                       | 0.05                   |
| 9         | 5          | TFT              | RT            | 72           | 70                       | 0.19                   |
| 10        | 5          | TFT              | 60            | 6            | > 99                     | 3.30                   |
| 11        | 2.5        | TFT              | 60            | 13           | 86                       | 2.64                   |
| <b>12</b> | <b>2.5</b> | <b>TFT</b>       | <b>70</b>     | <b>4.5</b>   | <b>&gt; 99</b>           | <b>8.80</b>            |
| 13        | 2.5        | TFT              | 80            | 4.5          | > 99                     | 8.80                   |

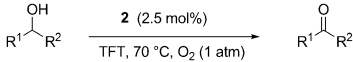
[a] Conditions: benzyl alcohol (1 mmol), O<sub>2</sub> (1 atm). [b] GC yield.

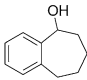
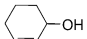
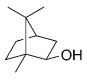
ing of 2.5 mol % in TFT as solvent at 70 °C are the best conditions for this system (Table 4, entry 12). Whereas the oxidation reaction proceeded well at room temperature in TFT (Table 4, entry 9), increasing the temperature to 70 °C resulted in significantly higher efficiency at lower catalyst loading, which led to the quantitative formation of benzaldehyde (Table 4, entries 9–12). It was also noted that the use of a higher reaction temperature is not beneficial for improving the reaction efficiency (Table 4, entry 13).

With optimized reaction conditions, we then investigated the applicability of our method with respect to other alcohol structures (Table 5). As shown in Table 5, a wide range of either primary or secondary benzylic alcohols were converted to their corresponding aldehydes or ketones in good to excellent yields (Table 5, entries 1–24). Notably, this method is highly selective for the oxidation of primary alcohols to their corresponding aldehydes without the formation of appreciable amounts of the corresponding carboxylic acids even after prolonged reaction times (Table 5, entries 1–11). Although substituted benzyl alcohols that contain electron-donating groups (such as CH<sub>3</sub>, OCH<sub>3</sub>, or *i*Pr; Table 5, entries 2–4) are more easily oxidized than those that bear electron-withdrawing groups (Table 5, entries 6–8), the substituents did not affect the selectivity of the process or the resulting deactivation of the catalyst. It is also worth noting that Ru@PMO-IL displays a high activity for the oxidation of secondary benzylic alcohols either cyclic or acyclic and gives their corresponding ketones in good to excellent yields with high selectivity (Table 5, entries 13–18). The catalyst Ru@PMO-IL was also found to be highly selective for the oxidation of organic substrates that contain C=C double bonds. Thus, primary and secondary allylic alcohols

were converted to their corresponding α,β-unsaturated carbonyl compounds in moderate to excellent yields (Table 5, entries 19–21). It is well known that aliphatic alcohols are more reluctant to undergo selective oxidation. Notably, Ru@PMO-IL was also capable of catalyzing the oxidation of these alcohols, although it was found that secondary aliphatic alcohols showed a higher activity than their primary counterparts (Table 5, entries 22–24).

It should also be noted that the same transformations for open-chain secondary alcohols when using our recently developed catalyst system (Au/Cs<sub>2</sub>CO<sub>3</sub>) were very sluggish and produced their corresponding ketones in poor yields (Table 5, entries 21 and 22).<sup>[57h]</sup> In the case of primary aliphatic and allylic alcohols, by increasing either the reaction time or reaction temperature so as to increase the conversion, selectivity towards the aldehyde decreases significantly on account of the overoxidation of the aldehyde to the corresponding carboxylic acid (Table 5, entries 19 and 22). Remarkably, sterically encumbered alcohols such as borneol were equally oxidized

Table 5. Aerobic oxidation of alcohols catalyzed by Ru@PMO-IL **2**.<sup>[a]</sup>


| Entry    | R <sup>1</sup>  | R <sup>2</sup>                                | <i>t</i> [h] | Yield [%] <sup>[b]</sup> | TOF [h <sup>-1</sup> ] |
|----------|---|---|--------------|--------------------------|------------------------|
| <b>1</b> | <b>C<sub>6</sub>H<sub>5</sub></b>   | <b>H</b>                                      | <b>4.5</b>   | <b>&gt; 99</b>           | <b>8.80</b>            |
| 2        | 4-Me-C <sub>6</sub> H <sub>4</sub>  | H   | 6.5          | > 99                     | 6.15                   |
| 3        | 4-MeO-C <sub>6</sub> H <sub>4</sub>   | H   | 4.0          | > 99                     | 10                     |
| 4        | 4- <i>i</i> Pr-C <sub>6</sub> H <sub>4</sub>  | H   | 8.5          | 95                       | 4.47                   |
| 5        | 4-Cl-C <sub>6</sub> H <sub>4</sub>  | H   | 6.0          | 95                       | 6.33                   |
| 6        | 3-Cl-C <sub>6</sub> H <sub>4</sub>  | H   | 17           | 99                       | 2.33                   |
| 7        | 2,6-Cl <sub>2</sub> -C <sub>6</sub> H <sub>3</sub>                                  | H   | 28           | 70                       | 0.99                   |
| 8        | 2-NO <sub>2</sub> -C <sub>6</sub> H <sub>4</sub>                                    | H   | 36           | 87                       | 0.96                   |
| 9        | 2,4-Cl-C <sub>6</sub> H <sub>3</sub>  | H   | 36           | 94                       | 1.04                   |
| 10       | 2-furyl   | H   | 22           | 91 <sup>[c]</sup>        | 1.18                   |
| 11       | cyclopropyl   | cyclopropyl                                   | 24           | 95 <sup>[c]</sup>        | 1.13                   |
| 12       | 3-pyridyl   | H   | 24           | 78 <sup>[d]</sup>        | 1.07                   |
| 13       | C <sub>6</sub> H <sub>5</sub>   | Me  | 5.5          | 96                       | 6.98                   |
| 14       | C <sub>6</sub> H <sub>5</sub>   | Et  | 6.5          | 91                       | 5.90                   |
| 15       |  |   | 24           | 65                       | 1.08                   |
| 16       | C <sub>6</sub> H <sub>5</sub>   | C <sub>6</sub> H <sub>5</sub> CH <sub>2</sub> | 33           | 91 <sup>[d]</sup>        | 0.55                   |
| 17       | C <sub>6</sub> H <sub>5</sub>   | C <sub>6</sub> H <sub>5</sub>                 | 24           | > 99 <sup>[d]</sup>      | 0.82                   |
| 18       | 4-MeO-C <sub>6</sub> H <sub>4</sub>   | 4-MeO-C <sub>6</sub> H <sub>4</sub>           | 15           | 92 <sup>[d]</sup>        | 1.22                   |
| 19       | Ph-CH=CH  | H   | 24           | 70                       | 1.16                   |
| 20       | Ph-CH=CH  | CH <sub>3</sub>                               | 12           | 90 <sup>[d]</sup>        | 1.50                   |
| 21       |  |   | 18           | 91                       | 2.02                   |
| 22       | Ph-CH <sub>2</sub> CH <sub>2</sub> CH <sub>2</sub>                                  | H   | 14           | 53 <sup>[d]</sup>        | 0.757                  |
| 23       | CH <sub>3</sub> (CH <sub>2</sub> ) <sub>5</sub>                                     | Me  | 33           | 75 <sup>[d]</sup>        | 0.45                   |
| 24       |  |   | 36           | 73 <sup>[d]</sup>        | 0.40                   |

[a] Conditions: alcohol (1 mmol), **2** (2.5 mol %), O<sub>2</sub> (1 atm), TFT (2 mL), at 70 °C unless otherwise stated. [b] GC yields using internal standard method. [c] Conditions: **2** (3.5 mol %), at 70 °C. [d] Conditions: **2** (5 mol %), at 85 °C.



to the corresponding ketone, although in these cases larger molar percentages of Ru were necessary (see footnotes to Table 5) to achieve high yields. Another important issue that can be understood from Table 5 is the remarkable activity of Ru@PMO-IL in promoting the aerobic oxidation of alcohols that contain heteroatoms such as oxygen, and nitrogen heterocycles, because the strong coordination of these alcohols to a metal center deactivate the catalyst. However, these alcohols could also be easily oxidized to their corresponding aldehydes in moderate to high yields under the optimized reaction conditions (Table 5, entries 10 and 12). Product analysis showed that selectivity decrease is a result of the overoxidation of aldehydes to carboxylic acids and also to the formation of an array of byproducts that are derived from the oxidative decomposition of the heterocycles. Even dicyclopentyl carbinol, which is remarkably sensitive, could also be oxidized to dicyclopentyl ketone in excellent yields in 24 h (Table 5, entry 11). The recyclability of **2** was also examined by separating it from the reaction mixture of the aerobic oxidation of benzyl alcohol through successive centrifugation, washing with toluene, and drying. In each run, the leaching of the Ru species into solution was negligible, as determined by inductively coupled plasma-atomic emission spectroscopy (ICP-AES) (lower than the detection limit of 1 ppm). Furthermore, no significant catalytic activity was observed from the residue of toluene extraction of **2** even after prolonged reaction times. The recycled catalyst was then used in five reaction cycles under the same reaction conditions (99, 99, 91, 89, and 75 %). The catalytic results indicate that a slight decrease in catalytic activity of the recovered catalyst for the aerobic oxidation was observed between the first and fourth runs. To clarify this issue, we also measured the Ru content of the recovered catalysts by means of ICP-AES. The average result of three individual experiments showed a Ru content of 0.30 and 0.29 mmol g<sup>-1</sup> for the fresh and the recovered catalyst, respectively. As can be seen, the amount of leached Ru in the recovered samples is negligible. This highlights the notion that the drop in catalytic activity might be mainly due to the loss of catalyst mass during the recycling and washing stages.

It is interesting to note that both N<sub>2</sub>-sorption analysis and transmission electron microscopy (TEM) showed that the ordered mesoporous structure of the PI-10 host matrix remained mostly unchanged after five runs of catalysis (Figure 6 and Figure S12 in the Supporting Information). Furthermore, TEM images of the recovered catalyst reveal that the Ru nanocluster with average diameters of 1.5–3.0 nm were well dispersed over the PMO-IL matrix (see the Supporting Information for high-resolution (HR) TEM images).

As the final part of this study, we were also very interested to compare the catalytic performance of our system to the ones already reported in the literature in terms of the observed turnover frequencies (TOFs; Table 6).

As can be clearly seen, the TOFs in our protocol are superior to those of the Ru-supported catalysts on carbon, hy-

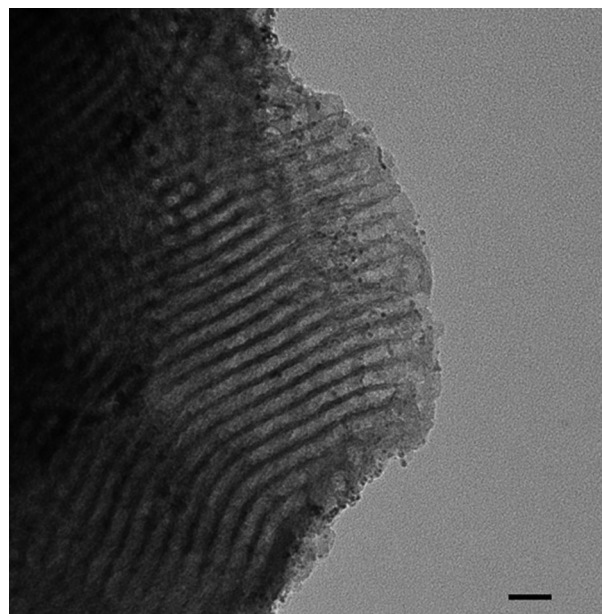


Figure 6. TEM image of the recovered catalyst after five reaction runs (scale bar: 20 nm).

droxyl apatite (HAP), MCM-41, and other types organic–inorganic hybrid Ru-based catalysts under nearly the same reaction conditions (Table 6, entries 1, 2, 5, 6, 9, and 10), whereas they are inferior to those obtained from Ru-supported catalysts on the inorganic oxides such as Al<sub>2</sub>O<sub>3</sub>, Fe<sub>3</sub>O<sub>4</sub>, and SiO<sub>2</sub> (Table 6, entries 3, 4, 7, 8, and 13 versus 15–18). It is very important to point out that a higher TOF of 23.2 h<sup>-1</sup> can be also obtained for our catalyst system based on the calculations that the Hutchings group<sup>[57b]</sup> used in 0.5 h reaction time for the same process. Given the excellent yields and selectivities and acceptably high TOFs obtained at lower reaction temperature using our catalyst system in the aerobic oxidation of a relatively wide range of alcohols, it is reasonable to consider this system a high-performance alternative for this purpose.

## Conclusion

In conclusion, a number of new alkyl imidazolium ionic-liquid-based periodic mesoporous organosilicas were synthesized by co-condensation of 1,3-bis[3-trimethoxysilylpropyl]imidazolium chloride and tetramethoxysilane (TMOS) by using a triblock copolymer templating approach in acidic media. PXRD, solid-state NMR spectroscopy, DRIFTS, nitrogen-sorption data, TEM images, and TGA analysis of the synthesized materials showed that ionic-liquid blocks are thoroughly incorporated into the wall mesostructures, and the PMO materials that contain 10–35 mol % IL have high surface area and narrow pore-size distributions with 2D hexagonal symmetry. Our studies showed that the structural properties and morphology of these materials strongly depend on the initial concentration of the precursor ionic



Table 6. Oxidation of some alcohols using different ruthenium catalysts.

| Entry | Alcohol             | Catalyst  | Mol % | <i>T</i> [°C] | <i>t</i> [h] | Yield [%] | Ref.               | TOF <sup>[a]</sup> [h <sup>-1</sup> ] |
|-------|---------------------|---|-------|---------------|--------------|-----------|--------------------|---------------------------------------|
| 1     | 1-phenyl ethanol    | HB Ru <sup>[b]</sup>                                | 5     | 110           | 9            | 98        | [55b]              | 2.17                                  |
| 2     | 4-Cl-benzyl alcohol | HB Ru   | 5     | 110           | 6            | 93        | [55b]              | 3.10                                  |
| 3     | 1-phenyl ethanol    | Ru/Al <sub>2</sub> O <sub>3</sub>                   | 2.5   | 83            | 1            | 99        | [59b]              | 39.60                                 |
| 4     | 4-Cl-benzyl alcohol | Ru/Al <sub>2</sub> O <sub>3</sub>                   | 2.5   | 83            | 1            | 99        | [59b]              | 39.60                                 |
| 5     | 1-phenyl ethanol    | Ru/HAP <sup>c</sup>                                 | 17    | 80            | 2            | 98        | [59a]              | 2.88                                  |
| 6     | 4-Cl-benzyl alcohol | Ru/HAP  | 17    | 80            | 3            | 99        | [59a]              | 1.94                                  |
| 7     | 1-phenyl ethanol    | Ru(OH) <sub>x</sub> /Fe <sub>3</sub> O <sub>4</sub> | 3.8   | 105           | 2            | 99        | [59e]              | 13.02                                 |
| 8     | 4-Cl-benzyl alcohol | Ru(OH) <sub>x</sub> /Fe <sub>3</sub> O <sub>4</sub> | 3.8   | 105           | 1            | 99        | [59e]              | 26.05                                 |
| 9     | 1-phenyl ethanol    | Ru/C  | 5     | 70            | 5            | 99        | [59h]              | 3.96                                  |
| 10    | 4-Cl-benzyl alcohol | Ru/C  | 5     | 50            | 6            | 82        | [59h]              | 2.73                                  |
| 11    | 1-phenyl ethanol    | RuO <sub>4</sub> <sup>-</sup> @MCM-41               | 1.3   | 80            | 24           | 100       | [59k]              | 3.20                                  |
| 12    | 4-Cl-benzyl alcohol | RuO <sub>4</sub> <sup>-</sup> @MCM-41               | 1.5   | 80            | 1            | quant     | [59k]              | -                                     |
| 13    | 1-phenyl ethanol    | RuO <sub>4</sub> <sup>-</sup> /SG <sup>[d]</sup>    | 10    | 75            | 0.16         | 98        | [59l]              | 61.25                                 |
| 14    | benzyl alcohol      | RuO <sub>4</sub> <sup>-</sup> /SG                   | 10    | 75            | 3            | 96        | [59l]              | 3.26                                  |
| 15    | 1-phenyl ethanol    | Ru@PMO-IL   | 2.5   | 70            | 5.5          | 96        | — <sup>[e]</sup>   | 6.9                                   |
| 16    | 4-Cl-benzyl alcohol | Ru@PMO-IL   | 2.5   | 70            | 6            | 95        | — <sup>[e]</sup>   | 6.3                                   |
| 17    | benzyl alcohol      | Ru@PMO-IL   | 2.5   | 70            | 4.5          | 99        | — <sup>[e]</sup>   | 8.8                                   |
| 18    | benzyl alcohol      | Ru@PMO-IL   | 2.5   | 70            | 0.5          | 29        | — <sup>[e,f]</sup> | 23.2                                  |

[a] All TOFs are calculated by this equation:  $\frac{1}{\text{cat. [mol\%]}} \times \frac{\text{yield [\%]}}{\text{time [h]}}$ . [b] Organic-inorganic hybrid ruthenium (HB Ru). [c] HAP = hydroxyapatite. [d] Sol-gel-encapsulated perruthenate. [e] The present protocol. [f] TOF was calculated after 0.5 h.

liquid (BTMSPI) in the synthetic solution. However, both PXRD and TEM studies revealed that the hexagonal ordering of the materials was retained over a relatively wide range of BTMSPI (10–35 molar percent of total silicon source). Diffraction patterns and nitrogen adsorption-desorption analyses of the as-prepared and solvent-extracted PMO-ILs also indicate outstanding solvothermal stability, because none of the samples exhibited any appreciable matrix contraction upon surfactant extraction. Given the unique character of the ordered mesoporous materials and ionic liquids, the described PMOs promise high-loading, stable, and tunable heterogeneous versions of ionic liquids for applications in different areas of nanotechnology, materials chemistry, catalysis, and chromatography. Further work on the practical applications of these materials as heterogeneous nanoreaction media and also as innovative supports for the immobilization of various types of transition-metal catalysts through anion-exchange capabilities of the materials is underway in our laboratories.

## Experimental Section

**Preparation of 1,3-bis(3-trimethoxysilylpropyl)imidazolium chloride (1):** IL **1** (see the Supporting Information) was synthesized by means of a modification of a literature procedure.<sup>[44]</sup> All reactions were carried out under an atmosphere of dry argon and all solvents were dried in the presence of suitable reagents and freshly distilled prior to use. Sodium imidazolide (90% purity, Fluka) and 3-chloropropyltrimethoxysilane (98%, Merck) were used as received. In a well-dried, two-necked 200 mL Schlenk flask, (3-chloropropyl)trimethoxysilane (8.11 g, 40.0 mmol) was added to a solution of sodium imidazolide (4.00 g, 40.0 mmol) in absolute THF (120 mL). The system was heated to reflux in the absence of light for 24 h and then allowed to cool to room temperature. After removal of solvent under vacuum, the resulting mixture was added to a solution of 3-chloropropyltrimethoxysilane (8.11 g, 40.0 mmol) in absolute toluene (120 mL). The reaction mixture was heated to reflux with exclusion of light for 48 h, and after cooling to room temperature, the supernatant sol-

ution was removed with a pipette. The resultant oil was first washed with absolute toluene (5 × 30 mL), and then CH<sub>2</sub>Cl<sub>2</sub> (50 mL) was added for the precipitation of NaCl from the reaction mixture. The solution in dichloromethane was transferred into another well-dried flask. Pale yellow IL **1** was obtained after removal of solvent and dried under vacuum at room temperature. <sup>1</sup>H NMR (250 MHz, CDCl<sub>3</sub>, 25 °C, TMS): δ = 10.00 (s, 1H; NCHN), 7.46 (d, <sup>3</sup>J = 1.7 Hz, 2H; CHCH), 4.32 (t, <sup>3</sup>J(H,H) = 7.1 Hz, 4H; NCH<sub>2</sub>), 3.60 (s, 18H; OCH<sub>3</sub>), 2.00 (m, 4H; CCH<sub>2</sub>C), 0.62 ppm (t, <sup>3</sup>J(H,H) = 8.1 Hz, 4H; SiCH<sub>2</sub>); <sup>13</sup>C NMR (63 MHz, CDCl<sub>3</sub>, 25 °C, TMS): δ = 136.1 (NCHN), 122.2 (CHCH), 51.8 (NCH<sub>2</sub>), 50.8 (OMe), 24.1 (CH<sub>2</sub>CH<sub>2</sub>CH<sub>2</sub>), 5.8 ppm (SiCH<sub>2</sub>).

**Synthesis of ionic-liquid-based periodic mesoporous organosilica (PMO-IL, PI-10) materials in the presence of triblock copolymer P123:** The synthetic procedure was mainly based on a previous report on the synthesis of the 1,4-diethylenebenzene-bridged PMOs.<sup>[43]</sup> Typically, P123 (1.58 g) and KCl (8.3 g) were dissolved in deionized water (9.9 g) and HCl solution (43.6 g, 2.0 M) with stirring at 40 °C for 3 h. A pre-prepared mixture (18.9 mmol) of tetramethoxysilane (TMOS) and IL in absolute methanol was added to this homogeneous solution and then stirred for 24 h at the same temperature. The resulting mixture was then transferred into a Teflon-lined autoclave and heated at 100 °C for 72 h under static conditions. The solid products were obtained by filtration, washed thoroughly with deionized water, and air-dried at room temperature. The surfactant was removed four times by Soxhlet extraction with ethanol (100 mL) and concentrated HCl (3 mL each time) for each sample (1 g) for 12 h. The resulting PMO materials were denoted as PI-*n*, for which *n* (*n* = 10, 25, 35, 50) is the mol % of IL in the initial mixture.

**Preparation of Ru@PMO-IL (2) catalyst:** Ru@PMO-IL was prepared on the basis of a simple ion-exchange technique according to a previous report.<sup>[62]</sup> For a typical method, PMO-IL (0.5 g, 1.0 mmol IL g<sup>-1</sup>) was added to deionized water (10 mL) and sonicated for at least 10 min. A solution of KRuO<sub>4</sub> (0.034 g, 0.016 mmol) in deionized water (3 mL) was gradually added to said suspension and stirred at room temperature for 5 h. The resulting system was filtered and washed with deionized water (3 × 10 mL) and acetone (2 × 10 mL), respectively. The resulting solid was dried at room temperature in vacuo. The loading of Ru was calculated to be 0.3 mmol g<sup>-1</sup> by means of ICP.

**General procedure for alcohol oxidation with Ru@PMO-IL (2):** Catalyst (80–160 mg, 2.5–5 mol % (with regard to substrate)) was added to a solution of alcohol (1 mmol) in TFT (2 mL), and then the suspension was heated at the 70 °C for the requisite time under an O<sub>2</sub> atmosphere (1 atm). The progress of the reaction was monitored by GC, and after the end of the reaction, the resulting mixture was cooled to room tempera-

ture. Finally, the catalyst was isolated with centrifugation, washed with toluene (2 × 10 mL), and dried under vacuum. The recovered catalyst was used in the recycling procedure in the same manner as reported in the first run.

## Acknowledgements

The authors thank the Institute for Advanced Studies in Basic Science (IASBS) and the Iran National Science Foundation (INSF) for supporting this work.

- [1] C. T. Kresge, M. E. Leonowicz, W. J. Roth, J. C. Vartuli, J. S. Beck, *Nature* **1992**, 359, 710–712.
- [2] J. S. Beck, J. C. Vartuli, W. J. Roth, M. E. Leonowicz, C. T. Kresge, K. D. Schmitt, C. T. W. Chu, D. H. Olson, E. W. Sheppard, S. B. McCullen, J. B. Higgins, J. L. Schlenker, *J. Am. Chem. Soc.* **1992**, 114, 10834–10843.
- [3] A. Sayari, S. Hamoudi, *Chem. Mater.* **2001**, 13, 3151–3168.
- [4] A. Stein, *Adv. Mater.* **2003**, 15, 763–775.
- [5] M. E. Davis, *Nature* **2002**, 417, 813–821.
- [6] E. L. Margelefsky, R. K. Zeidan, M. E. Davis, *Chem. Soc. Rev.* **2008**, 37, 1118–1126.
- [7] B. Hatton, K. Landskron, W. Whitnall, D. Perovic, G. A. Ozin, *Acc. Chem. Res.* **2005**, 38, 305–312.
- [8] W. J. Hunk, G. A. Ozin, *J. Mater. Chem.* **2005**, 15, 3716–3724.
- [9] S. Inagaki, S. Guan, Y. Fukushima, T. Ohsuna, O. Terasaki, *J. Am. Chem. Soc.* **1999**, 121, 9611–9614.
- [10] B. J. Melde, B. T. Holland, C. F. Blanford, A. Stein, *Chem. Mater.* **1999**, 11, 3302–3308.
- [11] T. Asefa, M. J. MacLachlan, N. Coombs, G. A. Ozin, *Nature* **1999**, 402, 867–871.
- [12] F. Hoffmann, M. Cornelius, J. Morell, M. Fröba, *Angew. Chem.* **2006**, 118, 3290–3328; *Angew. Chem. Int. Ed.* **2006**, 45, 3216–3251.
- [13] S. Fujita, S. Inagaki, *Chem. Mater.* **2008**, 20, 891–908.
- [14] O. Olkhovik, M. Jaroniec, *J. Am. Chem. Soc.* **2005**, 127, 60–61.
- [15] T. Asefa, M. J. MacLachlan, H. Grondy, N. Coombs, G. A. Ozin, *Angew. Chem.* **2000**, 112, 1878–1881; *Angew. Chem. Int. Ed.* **2000**, 39, 1808–1811.
- [16] S. Guan, S. Inagaki, T. Ohsuna, O. Terasaki, *J. Am. Chem. Soc.* **2000**, 122, 5660–5661.
- [17] J. R. Matos, M. Kruk, L. P. Mercuri, M. Jaroniec, T. Asefa, N. Coombs, G. A. Ozin, T. Kamiyama, O. Terasaki, *Chem. Mater.* **2002**, 14, 1903–1908.
- [18] T. Asefa, M. Kruk, M. J. MacLachlan, N. Coombs, H. Grondy, M. Jaroniec, G. A. Ozin, *J. Am. Chem. Soc.* **2001**, 123, 8520–8530.
- [19] Y. Goto, S. Inagaki, *Chem. Commun.* **2002**, 2410–2411.
- [20] M. P. Kapoor, Q. H. Yang, S. Inagaki, *J. Am. Chem. Soc.* **2002**, 124, 15176–15177.
- [21] J. Morell, J. Wolter, M. Fröba, *Chem. Mater.* **2005**, 17, 804–808.
- [22] G. Temtsin, T. Asefa, S. Bittner, G. A. Ozin, *J. Mater. Chem.* **2001**, 11, 3202–3206.
- [23] C. M. Li, H. Yang, X. Shi, R. Liu, Q. H. Yang, *Microporous Mesoporous Mater.* **2007**, 98, 220–226.
- [24] T. Welton, *Chem. Rev.* **1999**, 99, 2071–2084.
- [25] R. Sheldon, *Chem. Commun.* **2001**, 2399–2407.
- [26] Z. Conrad Zhang, *Adv. Catal.* **2006**, 49, 153–237.
- [27] T. Welton, *Coord. Chem. Rev.* **2004**, 248, 2459–2477.
- [28] A. E. Visser, R. P. Swatloski, W. M. Reichert, R. Mayton, S. Sheff, A. Wierzbicki, J. H. Davis, R. D. Rogers, *Chem. Commun.* **2001**, 135–136.
- [29] E. D. Bates, R. D. Mayton, I. Ntai, J. H. Davis, *J. Am. Chem. Soc.* **2002**, 124, 926–927.
- [30] D. B. Zhao, Y. C. Liao, Z. D. Zhang, *Clean Soil Air Water* **2007**, 35, 42–48.
- [31] A. Riisager, R. Fehrmann, S. Flicker, R. van Hal, M. Haumann, P. Wasserscheid, *Angew. Chem.* **2005**, 117, 826–830; *Angew. Chem. Int. Ed.* **2005**, 44, 815–819.
- [32] C. P. Mehnert, R. A. Cook, N. C. Dispenziere, M. Afeworki, *J. Am. Chem. Soc.* **2002**, 124, 12932–12933.
- [33] C. P. Mehnert, *Chem. Eur. J.* **2005**, 11, 50–56.
- [34] S. Abelló, F. Medina, X. Rodríguez, Y. Cesteros, P. Salagre, J. E. Su-eiras, D. Tichit, B. Coq, *Chem. Commun.* **2004**, 1096–1097.
- [35] X. D. Mu, J. Q. Meng, Z. C. Li, Y. Kou, *J. Am. Chem. Soc.* **2005**, 127, 9694–9695.
- [36] M. Gruttadauria, S. Riela, C. Aprile, P. Lo Meo, F. D’Anna, R. Noto, *Adv. Synth. Catal.* **2006**, 348, 82–92.
- [37] F. Shi, Q. H. Zhang, D. M. Li, Y. Q. Deng, *Chem. Eur. J.* **2005**, 11, 5279–5288.
- [38] M. Li, P. J. Pham, C. U. Pittman, T. Y. Li, *Microporous Mesoporous Mater.* **2009**, 117, 436–443.
- [39] A. Riisager, B. Jorgensen, P. Wasserscheid, R. Fehrmann, *Chem. Commun.* **2006**, 994–995.
- [40] Y. L. Gu, C. Ogawa, J. Kobayashi, Y. Mori, S. Kobayashi, *Angew. Chem.* **2006**, 118, 7375–7378; *Angew. Chem. Int. Ed.* **2006**, 45, 7217–7220.
- [41] B. Gadenne, P. Hesemann, J. J. E. Moreau, *Chem. Commun.* **2004**, 1768–1769.
- [42] B. Karimi, D. Enders, *Org. Lett.* **2006**, 8, 1237–1240.
- [43] B. Karimi, D. Elhamifar, J. H. Clark, A. J. Hunt, *Chem. Eur. J.* **2010**, 16, 8047–8053.
- [44] P. Nguyen, P. Hesemann, P. Gaveau, J. J. E. Moreau, *J. Mater. Chem.* **2009**, 19, 4164–4171.
- [45] C. S. J. Cazin, M. Veith, P. Braunstein, R. B. Bedford, *Synthesis* **2005**, 622–626.
- [46] M. Kruk, V. Antochshuk, J. R. Matos, L. P. Mercuri, M. Jaroniec, *J. Am. Chem. Soc.* **2002**, 124, 768–769.
- [47] M. C. Burleigh, M. A. Markowitz, M. S. Spector, B. P. Gaber, *J. Phys. Chem. B* **2001**, 105, 9935–9942.
- [48] A. Bordoloi, S. Sahoo, F. Lefebvre, S. B. Halligudi, *J. Catal.* **2008**, 259, 232–239.
- [49] Y. Jin, P. J. Wang, D. H. Yin, J. F. Liu, H. Y. Qiu, N. Y. Yu, *Microporous Mesoporous Mater.* **2008**, 111, 569–576.
- [50] W. P. Guo, D. C. Goh, X. S. Zhao, *J. Mater. Chem.* **2005**, 15, 4112–4114.
- [51] E. B. Cho, D. Kim, M. Jaroniec, *Langmuir* **2007**, 23, 11844–11849.
- [52] a) B. Karimi, A. Maleki, D. Elhamifar, J. H. Clark, A. J. Hunt, *Chem. Commun.* **2010**, 46, 6947–6949; b) B. Karimi, A. Maleki, *Chem. Commun.* **2009**, 5180–5182.
- [53] B. Karimi, D. Elhamifar, J. H. Clark, A. J. Hunt, *Org. Biomol. Chem.* **2011**, 9, 7420–7426.
- [54] M. Hudlicky, *Oxidation in Organic Chemistry*, ACS Monograph Series, American Chemical Society, Washington DC, **1990**.
- [55] a) R. A. Sheldon, J. K. Kochi, *Metal-Catalyzed Oxidation of Organic Compounds*, Academic Press, New York, **1984**; b) J.-E. Bäckvall, *Modern Oxidation Methods*, Wiley-VCH, Weinheim, **2004**. For recent review, see: c) B. Karimi, A. Zamani, *J. Iran. Chem. Soc.* **2008**, 5, 1–20; d) T. Matsumoto, M. Ueno, N. Wang, S. Kobayashi, *Chem. Asian J.* **2008**, 3, 196–214; e) T. Mallat, A. Baiker, *Chem. Rev.* **2004**, 104, 3037–3058; f) T. Punniyamurthy, S. Velusamy, J. Iqbal, *Chem. Rev.* **2005**, 105, 2329–2363.
- [56] a) K. Mori, K. Yamaguchi, T. Hara, T. Mizugaki, K. Ebitani, K. Kaneda, *J. Am. Chem. Soc.* **2002**, 124, 11572–11573; b) K. Mori, T. Hara, T. Mizugaki, K. Ebitani, K. Kaneda, *J. Am. Chem. Soc.* **2004**, 126, 10657–10666; c) B. Karimi, A. Zamani, J. H. Clark, *Organometallics* **2005**, 24, 4695–4698; d) B. Karimi, S. Abedi, J. H. Clark, V. Budarin, *Angew. Chem.* **2006**, 118, 4894–4897; *Angew. Chem. Int. Ed.* **2006**, 45, 4776–4779; e) B. Karimi, A. Zamani, S. Abedi, J. H. Clark, *Green Chem.* **2009**, 11, 109–119; f) Z. Hou, N. Theysen, A. Brinkmann, K. V. Klementiev, W. Grüner, M. Bühl, W. Schmidt, B. Spliethoff, B. Tesche, C. Weidenthaler, W. Leitner, *J. Catal.* **2008**, 258, 315–323; g) Z. Ma, H. Yang, Y. Qin, Y. Hao, G. Li, *J. Mol. Catal. A* **2010**, 331, 78–85.

- [57] a) A. Abad, C. Concepción, A. Corma, H. Garcia, *Angew. Chem.* **2005**, *117*, 4134–4137; *Angew. Chem. Int. Ed.* **2005**, *44*, 4066–4069; b) D. I. Enache, J. K. Edwards, P. London, B. Solsona-Espriu, A. F. Carley, A. A. Herzing, M. Watanabe, C. J. Kiely, D. W. Knight, G. J. Hutchings, *Science* **2006**, *311*, 362–365; c) F. Z. Su, Y. M. Liu, L. C. Wang, Y. Cao, H. Y. He, K. N. Fan, *Angew. Chem.* **2008**, *120*, 340–343; *Angew. Chem. Int. Ed.* **2008**, *47*, 334–337; d) T. Mitsudome, A. Noujima, T. Mizugaki, K. Jitsukawa, K. Kaneda, *Adv. Synth. Catal.* **2009**, *351*, 1890–1896; e) C. Lucchesi, T. Inasaki, H. Miyamura, R. Matsubara, S. Kobayashi, *Adv. Synth. Catal.* **2008**, *350*, 1996–2000; f) X. Wang, H. Kawanami, N. M. Islam, M. Chatterjee, T. Yokoyama, Y. Ikushima, *Chem. Commun.* **2008**, 4442–4444; g) H. Miyamura, R. Matsubara, Y. Miyazaki, S. Kobayashi, *Angew. Chem.* **2007**, *119*, 4229–4232; *Angew. Chem. Int. Ed.* **2007**, *46*, 4151–4154; h) B. Karimi, F. Kabiri Esfahani, *Chem. Commun.* **2009**, 5555–5557; i) H. Tsunoyama, H. Sakurai, Y. Negishi, T. Tsukuda, *J. Am. Chem. Soc.* **2005**, *127*, 9374–9375; j) S. Kanaoka, N. Yagi, Y. Fukuyama, S. Aoshima, H. Tsunoyama, T. Tsukuda, H. Sakurai, *J. Am. Chem. Soc.* **2007**, *129*, 12060–12061; k) S. Kim, S. W. Bae, J. S. Lee, J. Park, *Tetrahedron* **2009**, *65*, 1461–1466.
- [58] a) Y. M. A. Yamada, T. Arakawa, H. Hocke, Y. Uozumi, *Angew. Chem.* **2007**, *119*, 718–720; *Angew. Chem. Int. Ed.* **2007**, *46*, 704–706; b) T. Wang, C. X. Xiao, L. Yan, L. Xu, J. Luo, H. Shou, Y. Kou, H. Liu, *Chem. Commun.* **2007**, 4375–4377; c) H. Miyamura, R. Matsubara, S. Kobayashi, *Chem. Commun.* **2008**, 2031–2033; d) Y. H. Ng, S. Ikeda, Y. Morita, T. Harada, K. Ikeue, M. Matsumura, *J. Phys. Chem. C* **2009**, *113*, 12799–12805.
- [59] a) K. Yamaguchi, K. Mori, T. Mizugaki, K. Ebitani, K. Kaneda, *J. Am. Chem. Soc.* **2000**, *122*, 7144–7145; b) K. Yamaguchi, N. Mizuno, *Angew. Chem.* **2002**, *114*, 4720–4724; *Angew. Chem. Int. Ed.* **2002**, *41*, 4538–4542; c) B. Zhan, M. A. White, T.-K. Sham, J. A. Pincock, R. J. Doucet, K. V. Ramana Rao, K. N. Robertson, T. S. Cameron, *J. Am. Chem. Soc.* **2003**, *125*, 2195–2199; d) K. Ebitani, K. Motokura, T. Mizugaki, K. Kaneda, *Angew. Chem.* **2005**, *117*, 3489–3492; *Angew. Chem. Int. Ed.* **2005**, *44*, 3423–3426; e) M. Kotani, T. Koike, K. Yamaguchi, N. Mizuno, *Green Chem.* **2006**, *8*, 735–741; f) K. Mori, S. Kanai, T. Hara, T. Mizugaki, K. Ebitani, K. Jitsukawa, K. Kaneda, *Chem. Mater.* **2007**, *19*, 1249–1256; g) C. Mondelli, D. Ferri, A. Baiker, *J. Catal.* **2008**, *258*, 170–176; h) S. Mori, M. Takubo, K. Makida, T. Yanase, S. Aoyagi, T. Maegawa, Y. Monguchi, H. Sajiki, *Chem. Commun.* **2009**, 5159–5161; i) K. Yamaguchi, J. W. Kim, J. He, N. Mizuno, *J. Catal.* **2009**, *268*, 343–349; For excellent references on supported  $\text{RuO}_4^-$ , see: j) B. Hinzen, R. Lenz, S. V. Ley, *Synthesis* **1998**, 977–979; k) A. Bleloch, B. F. G. Johnson, S. V. Ley, A. J. Price, D. S. Shepard, A. W. Thomas, *Chem. Commun.* **1999**, 1907–1908; l) R. Ciriminna, M. Pagliaro, *Chem. Eur. J.* **2003**, *9*, 5067–5073; m) R. Ciriminna, P. Hesemann, J. J. E. Moreau, M. Carraro, S. Campestrini, M. Pagliaro, *Chem. Eur. J.* **2006**, *12*, 5220–5224.
- [60] a) K. Yamaguchi, N. Mizuno, *Angew. Chem.* **2003**, *15*, 1517; *Angew. Chem. Int. Ed.* **2003**, *42*, 1480; b) J. W. Kim, K. Yamaguchi, N. Mizuno, *Angew. Chem. Int. Ed.* **2008**, *47*, 9246; c) K. Yamaguchi, M. Matsushita, N. Mizuno, *Angew. Chem.* **2004**, *116*, 1602; *Angew. Chem. Int. Ed.* **2004**, *43*, 1576; d) K. Yamaguchi, T. Koike, M. Kotani, M. Matsushita, S. Shinachi, N. Mizuno, *Chem. Eur. J.* **2005**, *11*, 6574; e) J. W. Kim, T. Koike, M. Kotani, K. Yamaguchi, N. Mizuno, *Chem. Eur. J.* **2008**, *14*, 4104.
- [61] Loading of Ru catalyst was determined to be  $0.3 \text{ mmol g}^{-1}$  by ICP-AES.
- [62] B. Karimi, M. Ghoreishi-Nezhad, J. H. Clark, *Org. Lett.* **2005**, *7*, 625–628.

Received: February 4, 2012


Revised: June 25, 2012

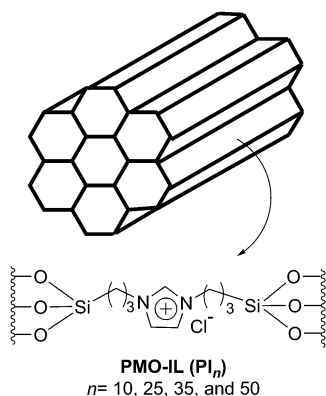
Published online: ■■■■, 0000



## Mesoporous Materials

B. Karimi,\* D. Elhamifar, O. Yari,  
M. Khorasani, H. Vali, J. H. Clark,  
A. J. Hunt ..... ■■■■-■■■■

 **Synthesis and Characterization of Alkyl Imidazolium Based Periodic Mesoporous Organosilicas: A Versatile Host for the Immobilization of Perruthenate ( $\text{RuO}_4^-$ ) in the Aerobic Oxidation of Alcohols**



**Go green:** The synthesis and characterization of a range of periodic mesoporous organosilica materials with different compositions of alkyl imidazolium ionic-liquid moieties (PMO-IL) is described (see scheme). As part of this study, the materials were also used for immobilization of perruthenate through an ion-exchange protocol. The resulting Ru@PI-10 was then employed as a recyclable catalyst.